Research Article

Nano Research
2024, 17(6): 5452–5460

ISSN 1998-0124 CN 11-5974/O4
https://doi.org/10.1007/s12274-024-6471-2

Quantitative assessment of the breast cancer marker HER2 using a gold nanoparticle-based lateral flow immunoassay

Liya Ye, Xinxin Xu, Aihua Qu, Liqiang Liu, Chuanlai Xu, and Hua Kuang (✉)

International Joint Research Laboratory for Biointerface and Biodetection, and School of Food Science and Technology, Jiangnan University, Wuxi 214122, China

Received: 29 November 2023 / **Revised:** 26 December 2023 / **Accepted:** 3 January 2024

ABSTRACT

Human epidermal growth factor receptor 2 (HER2) is an important biomarker for detection and treatment of breast cancer. In this study, we developed monoclonal antibodies against the extracellular domain (ECD) of HER2 and established a rapid and accurate lateral flow immunoassay (LFIA) for use in community medical institutions. The gene sequence of human HER2-ECD was obtained from the National Center for Biotechnology Information (NCBI) to construct the expression plasmid. HER2-ECD protein expressed in HEK293F cells was used to immunize BALB/c mice. The monoclonal antibodies were produced in mouse ascites and isolated by hybridoma cell screening. Antibodies were analyzed for purity by SDS-PAGE (sodium dodecyl sulphate-polyacrylamide gel-electrophoresis) and affinity was assessed by enzyme-linked immunosorbent assay (ELISA) while subtypes were detected using the commercial kits. The HER2-ECD test strip was prepared based on the sandwich method and evaluated using a portable detection instrument. The affinity of the paired antibodies, 4D8 and 8D9, both reached 1×10^8 L/mol. Both antibodies specifically recognized the HER2-ECD protein in serum. The limit of detection (LOD) of the gold nanoparticle (AuNP)-based LFIA was 1.7 ng/mL with a detection range of 1.7–400 ng/mL, and the performance of the HER2-ECD strip correlated well with that of a Siemens chemiluminescent immunoassay (CLIA) kit. In conclusion, the paired antibodies were successfully prepared with high affinity and specificity. The AuNP-based LFIA of HER2-ECD provides a fast and accurate method to detect the concentration of HER2-ECD in serum samples for clinical use in community medical institutions, and could contribute to determining the progress of the disease or the effectiveness of treatment.

KEYWORDS

human epidermal growth factor receptor 2, breast cancer, monoclonal antibody, quantitative, lateral flow immunoassay

1 Introduction

The human epidermal growth factor receptor family consists of four structurally-related members: HER1 (ErbB1, also known as epidermal growth factor receptor (EGFR)), HER2 (ErbB2), HER3 (ErbB3) and HER4 (ErbB4) [1, 2]. Among them, HER2 has gained increasing attention because of its important diagnostic value due to its overexpression or abnormal gene amplification in the tissues of patients with various tumors, especially breast cancer [3]. HER2 is a 185 kDa protein with an extracellular domain (ECD), a transmembrane domain, and an intracellular domain with tyrosine kinase activity [4, 5]. At present, breast cancer is the disease with the highest incidence among female malignant tumors worldwide [6–8]. Although there are many different methods for the diagnosis and treatment of breast cancer in the clinic, its incidence and mortality rate have not been significantly reduced, so how to improve the technical level of early diagnosis and prognosis assessment of breast cancer has become an urgent problem in the clinic. Approximately 25%–30% of breast cancer patients have HER2 overexpression [9, 10], and the analysis of HER2 expression in tumor tissue has been used as an independent indicator in the clinical diagnosis and treatment of tumors. The traditional methods of immunohistochemistry (IHC) and fluorescence *in situ* hybridization (FISH) for detecting HER2 expression in tumor tissues are invasive to normal tissues and do not allow for the detection of HER2 levels after surgery or for the monitoring of HER2 levels in patients [11]. In recent years, some studies have reported that there is a high concordance between the serum level of HER2-ECD in patients with breast tumors and the level of HER2 expression in their tissues [12], and that 50% or more of patients with metastatic breast cancer have elevated serum HER2 levels (relevant studies have shown that HER2 level of more than 15 ng/mL is indicative of tumor progression) [13, 14]. Hence, early detection of this biomarker and the development of effective diagnostic tests are of great importance.

At present, enzyme-linked immunosorbent assay (ELISA) is the most frequently-used method for the evaluation of serum HER2 levels in both clinical and experimental studies [15]. The HER2 ELISA has been commercialized by Siemens, and was approved by the Food and Drug Administration (FDA) in 2000 [16]. However, since ELISA includes different reaction methods which use different standards, the critical values of the elevated HER2 level are also different when determining the changes of HER2 level in the serum of breast cancer patients. Besides this, there are many studies on electrochemical detection methods [17–20]. Despite their high selectivity of biological recognition of the target analyte, these biosensors are expensive, time consuming and require

Address correspondence to kuangh@jiangnan.edu.cn

professional operation. Therefore, the development of a simple, fast, inexpensive, and safe biosensor holds great promise for identification of breast cancer HER2 subtypes as well as cancer prognosis. Nowadays, with the continuous progress of biotechnology, medical devices are developing in the direction of "simple, convenient and personal health management". Point–of–care testing (POCT) technology has become one of the hotspots for health monitoring with miniaturized size, easy operation and timely results [21–23], and lateral flow immunoassay (LFIA) is one of the most widely-used POCT technologies [24]. Colloidal gold is a nanoparticle with a surface double electric layer structure formed by chloroauric acid in the presence of a reducing agent. Colloidal gold is simple to prepare, stable in performance, has good biocompatibility, and can be combined with proteins, nucleic acids, etc. through non-covalent bonding. The labeling process is simple, convenient, and rapid, which has led to its widespread attention and application in the field of rapid diagnosis, thus making it an ideal choice for LFIA labels [25]. Traditional LFIAs provide only qualitative or semi-quantitative results by naked eye observation and can only be used to detect the presence of a specific biological component in a clinical sample at a concentration above that of the assay [26]. However, there are many analyses that require a quantitative element, such as monitoring changes in clinical indicators or determining the relative or absolute concentration of a specific analyte. With the development of optical detection instruments, immunochromatographic techniques combined with portable optical readers allow for highly-sensitive quantitative detection of targets [27–29].

In this work, a label-based HER2 immunosensor was developed based on sandwich protocols in which the biorecognition element (specific capture antibody) immobilized on a nitrocellulose (NC) membrane binds HER2, which is then quantified with the aid of a detection antibody labeled with colloidal gold. We chose to prepare custom monoclonal antibodies (mAbs) with the ability to selectively bind the target antigen with a high binding constant, thus giving our method better specificity and higher sensitivity. The structural HER2-ECD gene was expressed in a eukaryotic system. Monoclonal antibodies against the extracellular structural domain of HER2 were developed by hybridoma technology using the recombinant protein. The best pair among these antibodies was selected and screened for establishment of the LFIA method. After the detection of standard HER2 samples, we applied this AuNP-based LFIA to detect HER2 in serum samples, which indicated that the assay results were well correlated to those of chemiluminescent immunoassay (CLIA) kit tests.

2 Experimental

2.1 Materials and apparatus

HEK293F cells were purchased from Gibco (Thermo Fisher Scientific, Shanghai, China) and the SMM 293-TII expression medium used to culture this cell line was purchased from Sino Biological (Beijing, China). The SP2/0 myeloma cell line was purchased from the Chinese Academy of Sciences Cell Bank (Shanghai, China). Immune adjuvants, polyethylene glycol (PEG 1500), RPMI-1640 medium, fetal bovine serum (FBS), polyethylenimine (PEI, M_W ~ 25 kDa), bovine serum albumin (BSA), horseradish peroxidase (HRP) and goat anti-mouse IgG antibody were purchased from Merck Life Sciences (Shanghai, China). Ni-NTA and Protein G filler were purchased from Sangon Biotech Co., Ltd. (Shanghai, China). A mouse antibody subtype kit was purchased from Baiotong Experimental Material Center (Luoyang, China) and other reagents were purchased from Sinopharm Chemical Reagent Co., Ltd. (Shanghai, China). Polyvinylchloride backing (PVC, DB–6), absorbent pads (H5072), nitrocellulose membranes (Sartorius CN95) and sample pads (CB–SB08) were purchased from Shanghai Jieyi Biotechnology Co., Ltd. (Shanghai, China). The Airjet Quanti 3000™ dispenser was obtained from Xinqidian Gene Technology Co., Ltd. (Beijing, China). A hand–held strip scan reader was supplied by Huaan Magnech Bio-Tech Co., Ltd. (Beijing, China). The transmission electron microscope (TEM) was provided by the analytical platform of the University.

2.2 Ethical approval

Six-week-old BALB/c mice were purchased from Beijing Vital River Laboratory Animal Technology Co., Ltd. (Beijing, China). All animal procedures were performed in accordance with the Guidelines for Care and Use of Laboratory Animals of Jiangnan University and approved by the Animal Ethics Committee of Jiangnan University.

2.3 Expression and purification of HER2-ECD

There have been studies on the expression of the HER2-ECD using prokaryotic expression systems, especially *Escherichia coli*, but since prokaryotic expression systems cannot carry out post-translational folding, modification, and other processes, the expressed HER2-ECD may differ from the natural protein to a certain extent in terms of structure, function, and biological activity. It is known that the ECD of HER2 is highly glycosylated, so the use of *E. coli* to express the HER2-ECD cannot completely replicate its natural conformation, while instead, the use of eukaryotic systems to express the HER2-ECD for study theoretically has a higher degree of scientific validity in terms of biological structure and function. The HER2-ECD gene eukaryotic expression plasmid pCMV3–HER2-ECD (Fig. S1 in the Electronic Supplementary Material (ESM)) was synthesized by Nanjing Kingsley Biotechnology Co., Ltd. and was constructed by inserting the gene encoding the HER2-ECD (National Center for Biotechnology Information (NCBI) reference sequence: NP_004439.2, 23–642 aa), which was optimized for codons preferred by mammalian cells, into the eukaryotic expression vector pCMV3 with a 6× His tag [30]. The plasmid was extracted and purified and transfected into HEK293F cells, and the supernatant was collected by centrifugation after 72 h. Protein purification was carried out on a Ni^+ affinity chromatography column, using an eluent solution (20 mM Tris, 150 mM NaCl, 20, 50 and 250 mM imidazole, pH 8) for protein gradient elution, and the eluent at each imidazole concentration was collected. Finally, protein concentration after SDS-PAGE (sodium dodecyl sulphate-polyacrylamide gel-electrophoresis) analysis was quantified using a bicinchoninic acid (BCA) protein quantification kit [31].

2.4 Immunization, mAb production and purification

The monoclonal antibodies preparation process was shown in Fig. S2 in the ESM and the immunization schedule was similar to that of the previously-published reports [32–34]. Female BALB/c mice were immunized by subcutaneous multipoint injection of 100 μg/mouse. The first immunization was performed with Freund's complete adjuvant mixed with an equal volume of purified HER2-ECD and emulsified; subsequent immunizations were performed with Freund's incomplete adjuvant. Immunization was performed every 3 weeks for a total of four immunizations. Serum titer was measured by indirect ELISA at day 7 after each immunization starting from the second immunization, and the mouse with the highest serum titer was selected as the spleen donor [35, 36]. Hybridoma cells were produced by mixing SP2/0 cells and mouse spleen cells after booster immunization at a ratio of 1:10 by the

conventional PEG fusion method [37]. Indirect ELISA was used to identify positive wells capable of producing antibodies. The selected screened positive wells were subcloned by the limiting dilution method until the positive rate was 100%. Finally, hybridoma cell lines stably secreting anti-HER2-ECD monoclonal antibody were obtained and monoclonal antibody ascites were prepared in mice by the *in vivo* induction method. Ascites were collected and filtered through a 0.45 μm membrane, and purified using a protein G affinity chromatography column to obtain specific mAbs. Then, SDS-PAGE was used to analyze the purity of the antibodies.

2.5 Conjugation of the mAb to HRP

Conjugation of the mAb to HRP was performed as follows: Briefly, 0.2 mL of 10 mg/mL HRP and 0.2 mL of 0.06 M $NaIO_4$ were reacted for 30 min at 4 °C, and this caused the generation of aldehyde groups by oxidation of the hydroxyl groups on HRP. Next, 0.2 mL of 0.16 M glycol was added to the mixture to eliminate the excess $NaIO_4$ at room temperature. After this, 2 mg of purified mAb were added and the pH was adjusted to 9 by the addition of 0.05 M carbonate buffer, in which aldehyde groups could be linked to the amino groups of the antibody to produce the corresponding Schiff bases. After stirring for 20 h at 4 °C, a stable HRP–antibody conjugate was formed by adding 90 μL of 5 mg/mL $NaBH_4$ and precipitating by the addition of an equal volume of saturated ammonium sulfate solution. After centrifugation for 10 min at 5000*g*, the pellet was resuspended with 0.01 M PBS (pH 7.4). The HRP–antibody conjugate was dialyzed against 0.01 M PBS for 36 h at 4 °C and then added to an equal volume of glycerol, and stored at −20 °C for long-term storage. All the reactions, including the dialysis were protected from light and the HRP–antibody conjugate was characterized by direct ELISA. The purified mAbs and the HRP–mAb conjugates were then paired with each other in a sandwich ELISA format.

2.6 Pairwise analysis and affinity detection

To determine the optimal pairing of capture and detection antibodies, the obtained mAbs and the corresponding HRP-labeled mAbs were paired one by one using a double-antibody sandwich ELISA [38]. The mAbs were diluted to 4 μg/mL and then used to coat a 96-well plate at 100 μL/well and incubated at 37 °C for 2 h. The plate was washed three times with PBST (PBS containing 0.05% Tween-20), then 1% BSA was added at 200 μL/well, and the plate was blocked at 37 °C for 2 h. After blocking, 100 μL of HER2-ECD standard solution or 0.01 M PBS were added as positive and negative controls, respectively. Then, 100 μL of 4 μg/mL HRP-labeled mAb used as the detection antibody was added. The highest $OD_{450\ nm}$ ratio of the positive and negative controls (P/N value) was considered as the optimal combination.

The affinity constants (K_a) of the mAbs were determined by the reference method [39–41]. Indirect ELISA was performed by coating ELISA plates with HER2-ECD proteins at concentrations of 0.3, 0.1 and 0.03 μg/mL, and the mAbs were diluted in a 3-fold gradient starting from 0.3 μg/mL. The $OD_{450\ nm}$ values of each well were determined. Finally, the concentration of the mAbs was plotted as the horizontal coordinate and the $OD_{450\ nm}$ value as the vertical coordinate. The platform segment of the curve indicated that the antigen was fully bound, and the $OD_{450\ nm}$ value at this point was taken as 100% to determine the concentration of the mAb when the $OD_{450\ nm}$ value was 50%, which was calculated by substituting it into the Eq. (1) to obtain the K_a (L/mol).

$$K_a = (n-1)/(2\times(n\times[\text{Ab'}]t - [\text{Ab}]t)) \quad (1)$$

In this equation, n is the multiple of the antigen concentrations in each data set, and [Ab']t and [Ab]t are the corresponding mAb concentrations (mol/L). Furthermore, mAb subtypes were determined according to the instructions of the mouse subtype identification kit.

2.7 Preparation of gold nanoparticles (AuNPs) and optimization of key parameters

AuNPs were prepared by the trisodium citrate reduction method [42]. Briefly, in a clean 250 mL round-bottomed flask, 2 mL 1% chloroauric acid was diluted to 100 mL with deionized water, mixed using a magnetic stirrer with continuous stirring and heated to boiling, and at the same time, 3 mL of 1% trisodium citrate was rapidly added. The solution gradually changed from light yellow to grey-black and finally to burgundy, after which it continued to be heated for 10 min, then finally cooled to room temperature, and stored at 4 °C for further use.

To keep the LFIA in optimal working condition, we carried out experiments to optimize the volume of K_2CO_3 and the amounts of detection mAb for conjugation. First, we added 1 mL of colloidal gold solution into 1.5 mL eppendorf (EP) tubes, then added 6, 8, 10, 12, 14, 16, or 18 μL of 0.2 mol/L K_2CO_3 solution to each tube, and mixed well. An excess of 20 μL of detection mAb at a concentration of 1 mg/mL was then added, and after the antibody was well labeled with AuNPs, HER2-ECD was added for detection to observe the color development after which the result was read by a portable strip reader. To optimize the amount of mAb, it was added to the optimal pH colloidal gold solution at a final concentration of 2, 5, 10, 15, 20 or 25 μg/mL.

2.8 Construction and principle of LFIA strips for antigen detection based on AuNPs

As shown in Fig. 1, a single test strip consists of five components: sample pad, conjugate pad, absorbent pad, NC membrane, and PVC backing card. Sample pads were saturated with 0.01 mol/L PBS (containing 1% sucrose, 1% BSA, and 0.2% Tween-20) and dried at 37 °C for 3 h. Under optimal conditions, mAb-conjugated AuNPs were synthesized as previously described [43], sprayed onto a glass fiber membrane and dried at 37 °C overnight to obtain the conjugate pads. After diluting the capture mAb (2 mg/mL) and goat anti-mouse IgG (0.5 mg/mL) with PBS, they were subsequently sprayed onto the NC membrane to form the test line (T line) and control line (C line) using a scriber. Following this, the LFIA was assembled in the following order: The sample pad was first affixed onto the PVC plate, overlapping the conjugate pad by 2 mm, and the bottom of the antibody-coated NC membrane was then overlapped by 2 mm. Next, the absorbent pad was overlapped on top of the NC membrane by 2 mm. Finally, the assembled plate was cut into individual 3 mm wide test strips and stored in a desiccator for further experiments.

Figure 1 also shows the detection principle of the prepared AuNP-based LFIA. Goat anti-mouse IgG and the capture mAb were immobilized on the corresponding C line and T line. The sample solution migrated upward under capillary action to the absorbent pad. When the sample was negative, that is, the target analyte was not present in the sample, the AuNP-labeled detection mAb bound directly to the goat anti-mouse IgG, and only the C line appeared red. When the sample was positive, the AuNP-labeled detection mAb first bound to the target analyte, then moved forward under the capillary action and reacted with the capture mAb immobilized at the T-line to form a AuNP-labeled detection mAb–antigen–capture mAb complex, so that a large amount of colloidal gold accumulated at the T line, thus appearing red (positive). Excess AuNP-labeled mAb continued to bind to the goat anti-mouse IgG to form a red band. Therefore, if no color

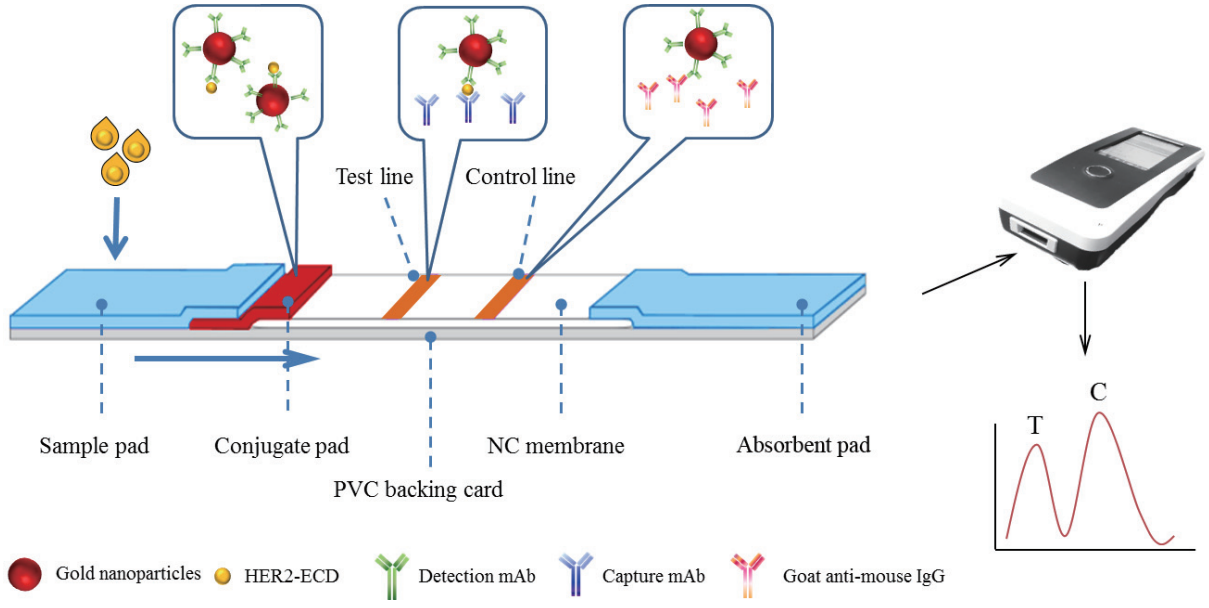

Figure 1 Schematic structure and principle of the AuNP–based LFIA strip.

was observed on the C line, the colloidal gold chromatography test strip was considered invalid. The immunochromatographic test strips were scanned with a portable reader and the color intensity of the C and T lines were recorded. The horizontal coordinate was the concentration of the standard solution of the target analyte, and the vertical coordinate was the T/C value (the ratio of the color intensity of the T line to the C line). A calibration curve was plotted using Origin 8.5 software for quantitative analysis, and then the color intensities of the samples were compared to the established calibration curve to calculate the concentration of the target analyte.

2.9 Performance of the LFIA strips

The HER2-ECD protein was diluted with healthy human serum to create standards of 10 concentration points, which were 0, 1.5, 3.1, 6.2, 12.5, 25.0, 50.0, 100.0, 200.0, and 400.0 ng/mL. The detection was carried out under optimal conditions, and the T/C value was measured using a quantitative detector. Each concentration was repeated three times, then the HER2-ECD concentration was plotted as the horizontal coordinate and the T/C value as the vertical coordinate, and fitted by the four-parameter method to plot the calibration curve. The sensitivity of the LFIA was evaluated in terms of the LOD. Following the American Society for Clinical and Laboratory Standards (CLSI) document EP17–A2 for the evaluation of the LOD, the test was performed using the diluted sample as the target, and the determination was repeated 20 times, the T/C values were measured, then the mean ($\bar{x}$) and the standard deviation (s) were obtained, and the concentration value corresponding to "$\bar{x} + 3 \times s$" was calculated according to the calibration curve [44, 45], which is the LOD of this method. The specificity of the LFIA was evaluated by analyzing four biomarkers, including procalcitonin (PCT), C-reactive protein (CRP), serum amyloid A (SAA), and interleukin-6 (IL-6) in the serum sample. In addition, the cross–reactivity of EGFR or HER1 with this reagent was analyzed.

2.10 Stability analysis

The prepared test strips were placed in an oven at 50 °C and tested at two-week intervals with two concentrations of 100 and 10 ng/mL, respectively. The test was repeated three times for each sample to compare the difference between the results of the high-temperature accelerated destructive reagent at 2nd, 4th, 6th, and 8th week and the control reagent (at 0th week).

2.11 Validation of the LFIA strips in real serum samples

In order to evaluate the precision and accuracy of the method, three batches of test strips were prepared, and different concentrations of standards were added to the negative samples, of 5, 50 and 200 ng/mL. Each concentration was repeated ten times, and the intra- and inter-sample coefficients of variation (*CV*s) and the mean recoveries of each concentration were calculated [46]. Finally, eighty clinical samples were tested in parallel with a Siemens Medical HER2 protein assay kit (chemiluminescent method), and correlation analysis was performed to evaluate the consistency of our newly-developed method with existing products on the market.

3 Results and discussion

3.1 Characterization of HER2-ECD and mAbs

The expression and purification of the recombinant HER2-ECD (Fig. 2(a)) were analyzed by SDS-PAGE, which showed that the protein was expressed in large amounts in the supernatant mainly in a soluble form, and its size of 110 KDa was consistent with the theoretical molecular weight. The concentration of purified HER2-ECD protein was determined by the BCA protein assay kit to be 1.2 mg/mL. Mice were immunized with this protein, and ten hybridoma cell lines secreting anti-HER2-ECD mAbs were screened by indirect ELISA after cell fusion, and named 1F3, 2C5, 3G8, 4D8, 5B9, 6G2, 7F2, 8D9, 9B9 and 10A7. As shown in Fig.

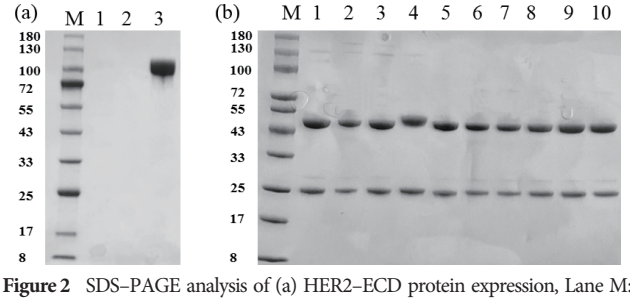

Figure 2 SDS–PAGE analysis of (a) HER2–ECD protein expression, Lane M: marker; Lane 1: eluent solution with 20 mM imidazole; Lane 2: eluent solution with 50 mM imidazole; Lane 3: eluent solution with 250 mM imidazole; and (b) ten mAbs, Lane M: marker; Lane 1: mAb 1F3; Lane 2: mAb 2C5; Lane 3: mAb 3G8; Lane 4: mAb 4D8; Lane 5: mAb 5B9; Lane 6: mAb 6G2; Lane 7: mAb 7F2; Lane 8: mAb 8D9; Lane 9: mAb 9B9; Lane 10: mAb 10A7.

2(b), the purified mAbs were analyzed by reduced SDS-PAGE, and there were obvious heavy chain bands and light chain bands at 50 and 25 kDa, respectively, and no obvious heterogeneous bands were seen, indicating that the mAbs were structurally intact and reached a higher purity after purification, and thus could be used in subsequent experiments.

3.2 Pairwise analysis

All the mAbs obtained were subjected to antibody pairing screening experiments using a checkerboard method, in which the higher P/N value indicated a better pairing. For the positive control, HER2-ECD was added at 50 ng/mL concentration (100 μL/well), and 100 μL of standard diluted solution (0.01 M PBS) was added as the negative control. As shown in Table 1, the highest P/N value was obtained using mAb 8D9 as the capture antibody and HRP-labeled mAb 4D8 as the detection antibody. This pair of mAbs was therefore selected for subsequent experiments on the establishment of the immunochromatographic detection method. The affinity constants of these mAbs were also determined and the K_a values were calculated. Among them, the affinity constants of 4D8 and 8D9 were higher, the K_a of 4D8 was 1.05×10^8 L/mol (Fig. 3(b)), and that of 8D9 was 1.02×10^8 L/mol (Fig. 3(c)), thus the affinity of this set of paired mAbs was obviously higher. Meanwhile, the results of antibody subtype analysis shown in Fig. 3(a) revealed that heavy chain of 8D9 was IgG2b while 4D8 was IgG1 and light chains were both κ chains.

3.3 Characterization of AuNPs and optimization of the LFIA

The prepared AuNPs were scanned using a UV–visible spectrophotometer over the wavelength range of 400–800 nm, with ultrapure water as the reference, and there was a maximum absorption peak at 528 nm, as shown in Fig. 4(a). Analysis by TEM showed that the colloidal gold particles produced were well dispersed with uniform particle size of around 30 nm, as shown in Fig. 4(b). This was consistent with the UV absorption peak of colloidal gold of 30 nm diameter reported in the literature, which is around 528 nm.

Current probes commonly wrap proteins on AuNPs by electrostatic adsorption, and the pH of their labeling reaction buffer and the surface chemistry of the AuNPs affect the adsorption efficiency and biological activity of the antibodies. The pH of the colloidal gold solution is generally adjusted by controlling the volume of K_2CO_3 solution during the labeling process. When the pH value is too low, crosslinking aggregation and sinking easily occur. In general, antibodies are maximally adsorbed to the gold surface when the pH value is equal to or slightly higher than the isoelectric point (pI) of the antibody (pI = 8). Therefore, 16 μL was selected as the optimal volume of K_2CO_3 for antibody coupling, and the pH value of the AuNP solution was approximately 8.5 (Fig. 5(a)).

The amount of antibody labeling is a critical factor affecting the detection ability of the test strips. An appropriate amount of antibody labeling facilitates the stability of the colloidal gold–antibody conjugate, while too much labeling may lead to a decrease in sensitivity. Our results (Fig. 5(b)) showed that the T/C value increased with increasing mAb concentration from 2 to 20 μg/mL. However, increasing the mAb to 25 μg/mL resulted in a decreased T/C value, implying that the excess antibody can reduce the binding affinity due to steric hindrance. Thus, the optimum mAb amount labeled on AuNPs was 20 μg/mL.

3.4 Sensitivity and specificity of the LFIA

In order for the quantitative test strips to be used in clinical applications, it was necessary to evaluate the performance of the established quantitative testing system. Serum samples containing different concentrations of HER2 were tested under optimal conditions using prepared immunochromatographic test strips. The calibration curve was plotted using the logarithm of HER2 concentration as the horizontal coordinate and the T/C value as the vertical coordinate. As shown in Fig. 6, the T/C value was proportional to the concentration of HER2-ECD protein within the detection range of 1.5–400 ng/mL, and exhibited a good linear relationship between the T/C value and the logarithm of HER2-ECD concentration for quantitative determination, which can be described by the following linear regression equation: $y = 0.2428 \times \ln(x) - 0.2317$, $R^2 = 0.97$. The LOD reflects the sensitivity of the detection system, and when the measured concentration of the substance is lower than the LOD, the detection system will not be able to accurately detect it. The assay was performed using diluted samples and was repeated 20 times to calculate the LOD of the LFIA as 1.7 ng/mL.

The specificity of the test strips was evaluated by their cross-reactivity with other common biomarkers in serum. As shown in Fig. 7, when the concentrations of EGFR, PCT, CRP, SAA and IL-6 were 1000 ng/mL, there was almost no signal response on the T-line of the test strips, and the T/C value of the test strips was negligible. In contrast, when the concentration of HER2-ECD in serum was 50 ng/mL, the T/C value of the test strips reached 0.85, indicating that the test strips were highly specific for the HER2-ECD and could be used for the specific detection of HER2-ECD in serum.

Table 1 The P/N value of pairwise interaction analysis using sandwich ELISA[a]

Detection mAbs	Capture mAbs									
	1F3	2C5	3G8	4D8	5B9	6G2	7F2	8D9	9B9	10A7
1F3–HRP	3.25	9.28	9.39	9.45	12.68	13.11	5.08	10.99	9.28	9.45
2C5–HRP	8.34	1.98	6.20	5.64	5.57	8.07	9.18	10.59	9.09	6.69
3G8–HRP	6.76	2.45	1.52	2.50	7.99	4.93	6.17	5.06	5.22	2.24
4D8–HRP	11.36	6.65	5.97	4.72	4.32	8.49	9.73	14.48	5.79	5.37
5B9–HRP	11.73	5.95	7.15	5.91	11.38	8.49	8.83	9.34	10.05	4.89
6G2–HRP	7.17	5.85	6.42	5.07	5.02	4.04	8.49	7.11	7.10	5.27
7F2–HRP	1.98	7.46	10.28	8.19	8.47	10.03	5.19	12.69	10.92	9.65
8D9–HRP	11.89	3.86	9.05	7.86	12.63	9.09	10.29	10.36	9.44	7.14
9B9–HRP	12.08	5.35	5.51	4.66	5.16	5.91	9.99	3.72	6.40	3.75
10A7–HRP	8.56	6.41	5.38	4.97	1.95	6.79	8.81	6.59	6.98	6.35

[a] P/N value was the ratio of $OD_{450\ nm}$ value of the positive to the negative control.

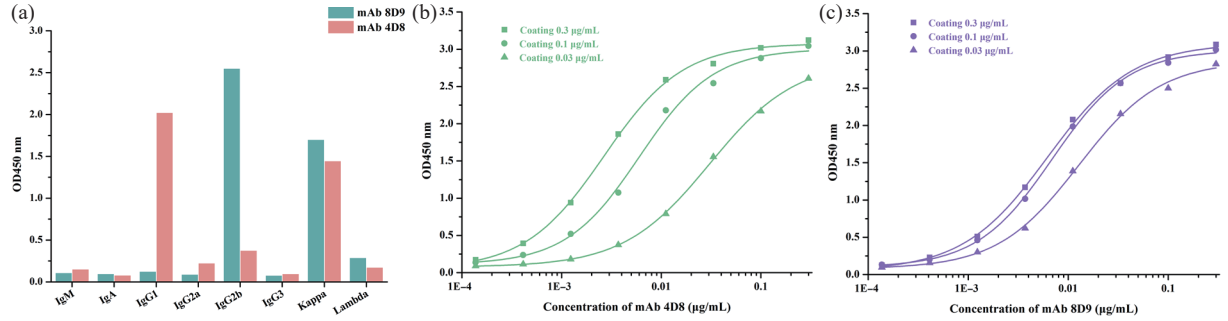

Figure 3 Characterization of the mAb obtained in our study. (a) Analysis of the subtype of mAb 4D8 and 8D9. (b) Affinity results of the mAb 4D8. (c) Affinity results of the mAb 8D9.

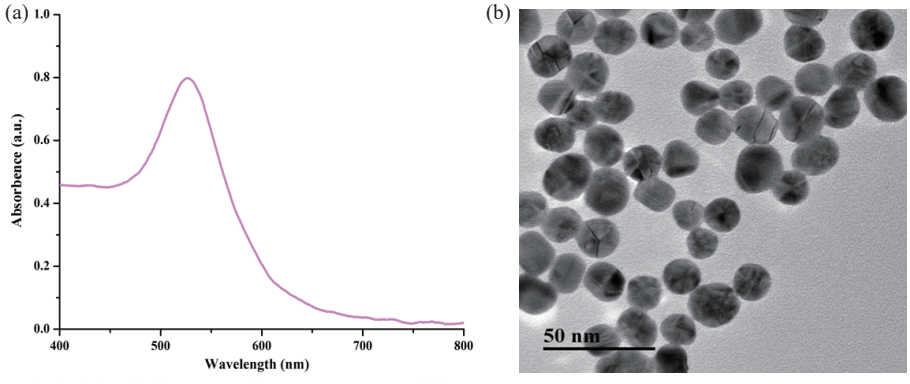

Figure 4 Characterization of colloidal gold: (a) UV–Vis absorption spectra and (b) TEM image.

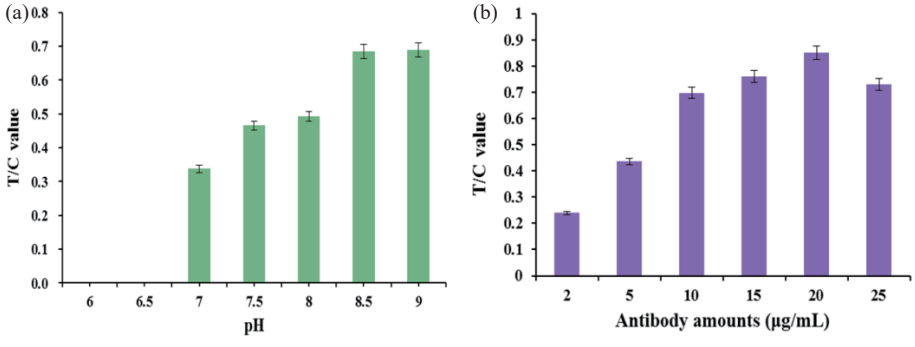

Figure 5 Optimization of (a) pH and (b) antibody amounts for the conjugation of mAb with AuNP.

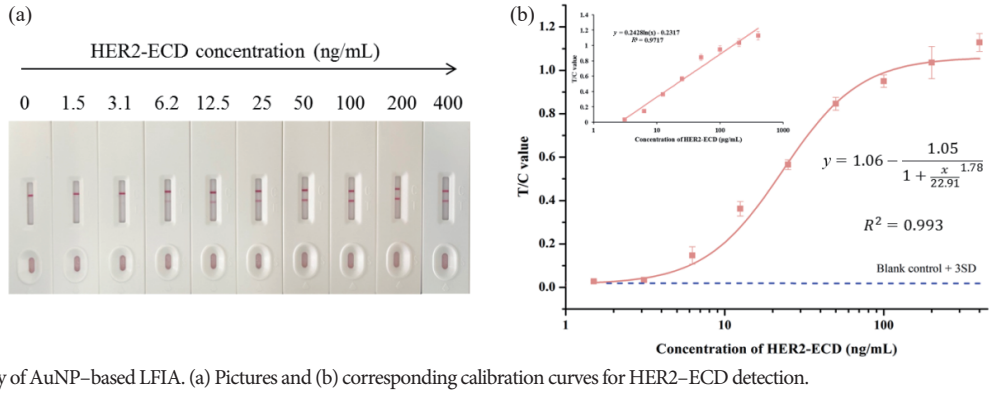

Figure 6 Sensitivity of AuNP–based LFIA. (a) Pictures and (b) corresponding calibration curves for HER2–ECD detection.

3.5 Accelerated stability

The results of the accelerated stability test at 50 °C were shown in Table 3, and the T/C values of the high and low concentration standards at 0th, 2nd, 4th, 6th and 8th week were consistent, indicating that the prepared test strips were stable for 8 weeks of accelerated destruction in 50 °C environment. According to the CLSI accelerated stability evaluation procedure [47], the validity of this test strip is predicted to be up to 18 months at room temperature (25 °C).

3.6 Validation of the detection performance of the LFIA

HER2-ECD was added to serum at 5, 50 and 200 ng/mL, and the assay was repeated ten times for each concentration, and the results are shown in Table 2. The intra– and inter–batch recoveries ranged from 92.0% to 105.3%, with CVs lower than 10.0%, indicating that the quantitative test strips have good accuracy and precision in the detection of serum HER2-ECD.

The accuracy and reliability of the quantitative test strips for detecting actual clinical samples were further evaluated. Eighty

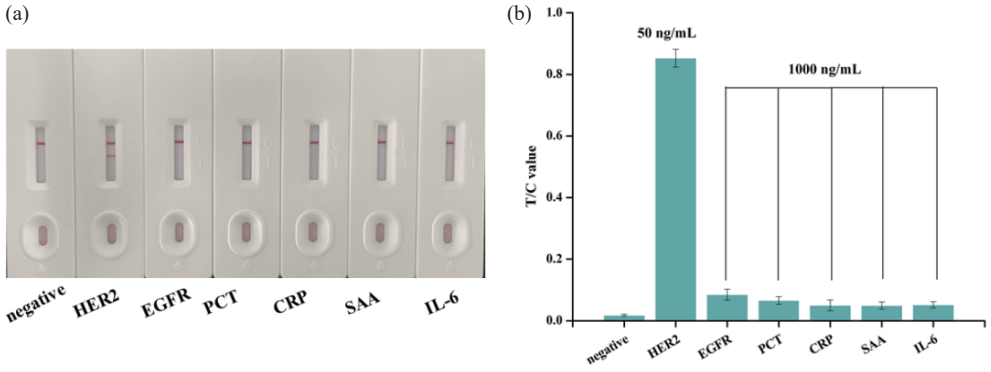

Figure 7 Specificity of AuNP–based LFIA. (a) Pictures and (b) corresponding T/C values of the strips.

Table 2 Accuracy and precision of the AuNP–based strips in serum

HER2–ECD concentration(ng/mL)	Intra–assay			Inter–assay[a]		
	Mean[b]	Recovery (%)	CV (%)	Mean	Recovery (%)	CV (%)
5	5.1	102.0	5.9	4.6	92.0	6.2
50	47.7	95.4	7.3	52.5	105.0	8.6
200	210.5	105.3	3.4	208.3	104.2	7.1

[a] Assay was completed every day for three days continuously.

[b] Mean value of ten replicates at each diluted concentration.

Table 3 The results of accelerated stability

		Week 0	Week 2	Week 4	Week 8
		T/C	T/C	T/C	T/C
100 ng/mL	1	0.886	0.828	0.847	0.839
	2	0.905	0.888	0.897	0.863
	3	0.864	0.894	0.843	0.873
10 ng/mL	1	0.327	0.311	0.396	0.329
	2	0.368	0.351	0.379	0.392
	3	0.368	0.343	0.303	0.338

HER2 serum samples were collected from Yixing People's Hospital, Jiangsu Province, China. The results were compared between the test strips prepared in this study and a commercially-available CLIA kit. As shown in Fig. 8, the good consistency between the two methods for the detection of HER2 in serum samples indicates that the test strips are practical and reliable for the detection of HER2 in real samples, and can be used for the rapid detection of HER2 in clinical serum samples. Compared with the traditional CLIA kits, the test strips based on obtained mAbs prepared in this study have obvious advantages in terms of detection time, cost and suitability for use as a home self-test.

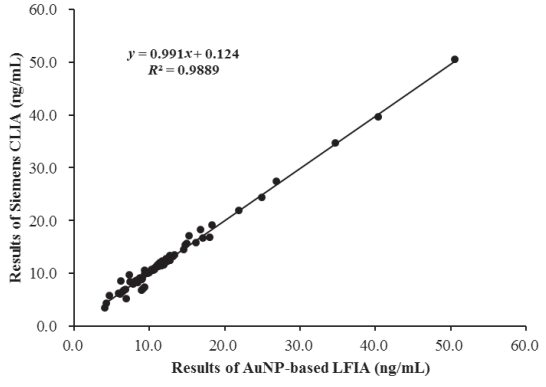

Figure 8 Correlation analysis of HER2–ECD protein between AuNP–based LFIA and Siemens CLIA kit.

4 Conclusions

Currently, HER2 detection methods based on histologic methods include IHC and FISH, among others. However, there is an urgent need to develop simpler methods for dynamic monitoring of the course and treatment outcome of HER2-positive breast cancer patients. In a retrospective study of serum and tissue samples from breast cancer patients before and after treatment and at different stages, researchers found that patients with early-stage breast cancer were negative for serum HER2, and that increases or decreases in serum HER2 of more than 20% were associated not only with disease progression but also with treatment outcomes. A study of serum and tissue samples from patients with different stages of primary breast cancer found that serum HER2 levels were highly consistent with the intracellular/extracellular segments of HER2 in tumor tissues, suggesting that there is a scientific basis for measuring the levels of HER2 in the serum of patients with tumors as a criterion for the diagnosis of the tumor as well as the formulation of the treatment plan, and that its trend of change can be used as a prognostic indicator for the evaluation of patients with tumors. In addition, the detection of HER2 protein levels in serum can avoid the harm caused by tissue biopsy and provide dynamic monitoring of recurrent or metastatic tumors to assist in determining the course of the disease or the efficacy of treatment.

In this study, the expression of recombinant HER2-ECD protein was carried out through a eukaryotic expression system. Because the post-translational processing and modification system

of mammalian cells are more complete, the expressed exogenous proteins are closer to their natural conformation, and thus can be immunized to obtain antibodies with higher specificity and affinity. The recombinant protein was used to immunize mice, and the paired monoclonal antibodies 8D9 and 4D8 were obtained, both of which had an affinity of 1×10^8 L/mol and were able to specifically recognize HER2 in human blood. The immunochromatographic assay established in this study used colloidal gold as the tracer, and the performance evaluation showed that the detection range of the assay was 1.7–400 ng/mL, with good reproducibility, a result in good agreement with that of the Siemens HER2 assay kit. In summary, this LFIA has the characteristics of short detection time, simple operation, high automation, high reproducibility and accuracy, and good specificity, and thus has great prospects for application and promotion. However, it is still necessary to collect relevant clinical data to evaluate its clinical efficacy, to provide a reference for further optimizing the detection of serum HER2 protein, and to provide technological support for enhancing the diagnostic and therapeutic effects of breast cancer.

Acknowledgements

This work is financially supported by the National Natural Science Foundation of China (No. 22236002), and National Key R&D Program(Nos. 2023YFF1105003 and 2022YFA1207300).

Electronic Supplementary Material: Supplementary material (further details of the schematic diagrams of plasmid and monoclonal antibodies preparation process) is available in the online version of this article https://doi.org/10.1007/s12274-024-6471-2.

References

[1] Wieduwilt, M. J.; Moasser, M. M. The epidermal growth factor receptor family: Biology driving targeted therapeutics. *Cell. Mol. Life Sci.* **2008**, *65*, 1566–1584.

[2] Yarden, Y.; Sliwkowski, M. X. Untangling the ErbB signalling network. *Nat. Rev. Mol. Cell. Biol.* **2001**, *2*, 127–137.

[3] Slamon, D. J.; Clark, G. M.; Wong, S. G.; Levin, W. J.; Ullrich, A.; McGuire, W. L. Human breast cancer: Correlation of relapse and survival with amplification of the HER-2/*neu* oncogene. *Science* **1987**, *235*, 177–182.

[4] Akiyama, T.; Sudo, C.; Ogawara, H.; Toyoshima, K.; Yamamoto, T. The product of the human c-*erb*B-2 gene: A 185-kilodalton glycoprotein with tyrosine kinase activity. *Science* **1986**, *232*, 1644–1646.

[5] Rubin, I.; Yarden, Y. The basic biology of HER2. *Ann. Oncol.* **2001**, *12*, S3–S8.

[6] Ligibel, J. A. Could the women's health initiative breathe new life into breast cancer prevention. *J. Clin. Oncol.* **2020**, *38*, 1375–1377.

[7] Kamgar, M.; Assad, H.; Hastert, T. A.; McLaughlin, E.; Reding, K.; Paskett, E. D.; Bea, J. W.; Shadyab, A. H.; Neuhouser, M. L.; Nassir, R. et al. Peripheral neuropathy after breast cancer: An analysis of data from the women's health initiative life and longevity after cancer cohort. *J. Clin. Oncol.* **2020**, *38*, e24093.

[8] Papakonstantinou, A.; Nuciforo, P.; Borrell, M.; Zamora, E.; Pimentel, I.; Saura, C.; Oliveira, M. The conundrum of breast cancer and microbiome - a comprehensive review of the current evidence. *Cancer Treat. Rev.* **2022**, *111*, 102470.

[9] Wolff, A. C.; Hammond, M. E. H.; Allison, K. H.; Harvey, B. E.; Mangu, P. B.; Bartlett, J. M. S.; Bilous, M.; Ellis, I. O.; Fitzgibbons, P.; Hanna, W. et al. Human epidermal growth factor receptor 2 testing in breast cancer: American society of clinical oncology/college of american pathologists clinical practice guideline focused update. *Arch. Pathol. Lab. Med.* **2018**, *142*, 1364–1382.

[10] Xu, B.; Shen, J. G.; Guo, W. H.; Zhao, W. H.; Zhuang, Y. Y.; Wang, L. B. Impact of the 2018 ASCO/CAP HER2 guidelines update for HER2 testing by FISH in breast cancer. *Pathol. Res. Pract.* **2019**, *215*, 251–255.

[11] Perez, E. A.; Cortés, J.; Gonzalez-Angulo, A. M.; Bartlett, J. M. S. HER2 testing: Current status and future directions. *Cancer Treat. Rev.* **2014**, *40*, 276–284.

[12] Shamshirian, A.; Aref, A. R.; Yip, G. W.; Ebrahimi Warkiani, M.; Heydari, K.; Razavi Bazaz, S.; Hamzehgardeshi, Z.; Shamshirian, D.; Moosazadeh, M.; Alizadeh-Navaei, R. Diagnostic value of serum HER2 levels in breast cancer: A systematic review and meta-analysis. *BMC Cancer.* **2020**, *20*, 1049.

[13] Lam, L.; McAndrew, N.; Yee, M.; Fu, T.; Tchou, J. C.; Zhang, H. T. Challenges in the clinical utility of the serum test for HER2 ECD. *Biochim. Biophys. Acta Rev. Cancer.* **2012**, *1826*, 199–208.

[14] Tsé, C.; Gauchez, A. S.; Jacot, W.; Lamy, P. J. HER2 shedding and serum HER2 extracellular domain: Biology and clinical utility in breast cancer. *Cancer Treat. Rev.* **2012**, *38*, 133–142.

[15] Alhalwani, A. Y.; Repine, J. E.; Knowles, M. K.; Huffman, J. A. Development of a sandwich ELISA with potential for selective quantification of human lactoferrin protein nitrated through disease or environmental exposure. *Anal. Bioanal. Chem.* **2018**, *410*, 1389–1396.

[16] Moelans, C. B.; de Weger, R. A.; Van der Wall, E.; van Diest, P. J. Current technologies for HER2 testing in breast cancer. *Crit. Rev. Oncol. Hematol.* **2011**, *80*, 380–392.

[17] Ahirwar, R. Recent advances in nanomaterials-based electrochemical immunosensors and aptasensors for HER2 assessment in breast cancer. *Microchim. Acta* **2021**, *188*, 317.

[18] Lah, Z. M. A. N. H.; Ahmad, S. A. A.; Zaini, M. S.; Kamarudin, M. A. An electrochemical sandwich immunosensor for the detection of HER2 using antibody-conjugated PbS quantum dot as a label. *J. Pharm. Biomed. Anal.* **2019**, *174*, 608–617.

[19] Freitas, M.; Nouws, H. P. A.; Keating, E.; Delerue-Matos, C. High-performance electrochemical immunomagnetic assay for breast cancer analysis. *Sens. Actuators B Chem.* **2020**, *308*, 127667.

[20] Marques, R. C. B.; Viswanathan, S.; Nouws, H. P. A.; Delerue-Matos, C.; González-García, M. B. Electrochemical immunosensor for the analysis of the breast cancer biomarker HER2 ECD. *Talanta* **2014**, *129*, 594–599.

[21] Chu, H. W.; Liu, C. H.; Liu, J. S.; Yang, J.; Li, Y. C.; Zhang, X. J. Recent advances and challenges of biosensing in point-of-care molecular diagnosis. *Sens. Actuators B Chem.* **2021**, *348*, 130708.

[22] Yang, J. C.; Wang, K.; Xu, H.; Yan, W. Q.; Jin, Q. H.; Cui, D. X. Detection platforms for point-of-care testing based on colorimetric, luminescent and magnetic assays: A review. *Talanta* **2019**, *202*, 96–110.

[23] Zhu, G. Y.; Yin, X. D.; Jin, D. L.; Zhang, B.; Gu, Y. Y.; An, Y. R. Paper-based immunosensors: Current trends in the types and applied detection techniques. *Trends Analyt. Chem.* **2019**, *111*, 100–117.

[24] Mahmoudi, T.; de la Guardia, M.; Baradaran, B. Lateral flow assays towards point-of-care cancer detection: A review of current progress and future trends. *Trends Analyt. Chem.* **2020**, *125*, 115842.

[25] Lou, D. D.; Fan, L.; Jiang, T.; Zhang, Y. Advances in nanoparticle-based lateral flow immunoassay for point-of-care testing. *VIEW* **2022**, *3*, 20200125.

[26] Nguyen, V. T.; Song, S.; Park, S.; Joo, C. Recent advances in high-sensitivity detection methods for paper-based lateral-flow assay. *Biosens. Bioelectron.* **2020**, *152*, 112015.

[27] Jiang, N.; Ahmed, R.; Damayantharan, M.; Ünal, B.; Butt, H.; Yetisen, A. K. Lateral and vertical flow assays for point-of-care diagnostics. *Adv. Healthc. Mater.* **2019**, *8*, 1900244.

[28] Urusov, A. E.; Zherdev, A. V.; Dzantiev, B. B. Towards lateral flow quantitative assays: Detection approaches. *Biosensors* **2019**, *9*, 89.

[29] Lu, Z. D.; O'Dell, D.; Srinivasan, B.; Rey, E.; Wang, R. S.; Vemulapati, S.; Mehta, S.; Erickson, D. Rapid diagnostic testing platform for iron and vitamin A deficiency. *Proc. Natl. Acad. Sci. USA* **2017**, *114*, 13513–13518.

[30] Ye, L. Y.; Xu, L. G.; Kuang, H.; Xu, X. X.; Xu, C. L. Colloidal gold-based immunochromatographic biosensor for quantitative detection of S100B in serum samples. *Nanoscale Horiz.* **2023**, *8*, 1253–1261.

[31] Ye, L. Y.; Xu, X. X.; Song, S. S.; Xu, L. G.; Kuang, H.; Xu, C. L.

Rapid colloidal gold immunochromatographic assay for the detection of SARS-CoV-2 total antibodies after vaccination. *J. Mater. Chem. B* **2022**, *10*, 1786–1794.
[32] Ye, L. Y.; Lei, X. L.; Xu, L. G.; Kuang, H.; Xu, C. L.; Xu, X. X. Gold nanoparticle-based immunochromatographic assay for the rapid detection of the SARS-CoV-2 Omicron variant. *Mater. Chem. Front.* **2023**, *7*, 4063–4072.
[33] Guo, L. L.; Xu, X. X.; Zhao, J.; Hu, S. D.; Xu, L. G.; Kuang, H.; Xu, C. L. Multiple detection of 15 triazine herbicides by gold nanoparticle based-paper sensor. *Nano Res.* **2022**, *15*, 5483–5491.
[34] Lei, X. L.; Xu, X. X.; Wang, L.; Zhou, W.; Liu, L. Q.; Xu, L. G.; Kuang, H.; Xu, C. L. A quadruplex immunochromatographic assay for the ultrasensitive detection of 11 anesthetics. *Nano Res.* **2023**, *16*, 11269–11277.
[35] Zeng, L.; Xu, X. X.; Song, S. S.; Xu, L. G.; Liu, L. Q.; Xiao, J.; Xu, C. L.; Kuang, H. Synthesis of haptens and gold-based immunochromatographic paper sensor for vitamin B6 in energy drinks and dietary supplements. *Nano Res.* **2022**, *15*, 2479–2488.
[36] Lei, X. L.; Xu, X. X.; Liu, L. Q.; Xu, L. G.; Wang, L.; Kuang, H.; Xu, C. L. Gold-nanoparticle-based multiplex immuno-strip biosensor for simultaneous determination of 83 antibiotics. *Nano Res.* **2023**, *16*, 1259–1268.
[37] Yu, X. C.; McGraw, P. A.; House, F. S.; Crowe, J. E. An optimized electrofusion-based protocol for generating virus-specific human monoclonal antibodies. *J. Immunol. Methods* **2008**, *336*, 142–151.
[38] Zeng, L.; Guo, L. L.; Wang, Z. X.; Xu, X. X.; Ding, H. L.; Song, S. S.; Xu, L. G.; Kuang, H.; Xu, C. L. Gold nanoparticle-based immunochromatographic assay for detection *Pseudomonas aeruginosa* in water and food samples. *Food Chem. X* **2021**, *9*, 100117.
[39] Liu, J. J.; Cui, D. X.; Jiang, Y.; Li, Y. Y.; Liu, Z. X.; Tao, L.; Zhao, Q.; Diao, A. P. Selection and characterization of a novel affibody peptide and its application in a two-site ELISA for the detection of cancer biomarker alpha-fetoprotein. *Int. J. Biol. Macromol.* **2021**, *166*, 884–892.
[40] Guliy, O. I.; Velichko, N. S.; Fedonenko, Y. P.; Bunin, V. D. Use of an electro-optical sensor and phage antibodies for immunodetection of *Herbaspirillum*. *Talanta* **2019**, *202*, 362–368.
[41] Wang, Z. X.; Wu, X. L.; Liu, L. Q.; Xu, L. G.; Kuang, H.; Xu, C. L. An immunochromatographic strip sensor for sildenafil and its analogues. *J. Mater. Chem. B* **2019**, *7*, 6383–6389.
[42] Lu, Q. Q.; Ding, H. L.; Liu, L. Q.; Xu, L. G.; Kuang, H.; Xu, C. L.; Guo, L. L. Immunochromatographic assay for rapid detection of flupyradifurone in grape, blueberry, and tomato samples. *Food Chem.* **2024**, *433*, 137328.
[43] Liu, J.; Xu, X. X.; Wu, A. H.; Song, S. S.; Xu, L. G.; Xu, C. L.; Kuang, H.; Liu, L. Q. Immunochromatographic assay for the rapid and sensitive detection of etoxazole in orange and grape samples. *LWT* **2022**, *163*, 113519.
[44] Han, H.; Wang, C. W.; Yang, X. S.; Zheng, S.; Cheng, X. D.; Liu, Z. Z.; Zhao, B. H.; Xiao, R. Rapid field determination of SARS-CoV-2 by a colorimetric and fluorescent dual-functional lateral flow immunoassay biosensor. *Sens. Actuators B Chem.* **2022**, *351*, 130897.
[45] Wang, C. W.; Yang, X. S.; Zheng, S.; Cheng, X. D.; Xiao, R.; Li, Q. J.; Wang, W. Q.; Liu, X. X.; Wang, S. Q. Development of an ultrasensitive fluorescent immunochromatographic assay based on multilayer quantum dot nanobead for simultaneous detection of SARS-CoV-2 antigen and influenza A virus. *Sens. Actuators B Chem.* **2021**, *345*, 130372.
[46] Zhou, S.; Peng, Y. L.; Hu, J.; Duan, H.; Ma, T. T.; Hou, L.; Li, X. M.; Xiong, Y. H. Quantum dot nanobead-based immunochromatographic assay for the quantitative detection of the procalcitonin antigen in serum samples. *Microchem. J.* **2020**, *159*, 105533.
[47] Geistanger, A.; Braese, K.; Laubender, R. Automated data analytics workflow for stability experiments based on regression analysis. *J. Mass. Spectrom Adv. Clin. Lab.* **2022**, *24*, 5–14.